Biochimica et Biophysica Acta 1787 (2009) 144–154

Contents lists available at ScienceDirect

Biochimica et Biophysica Acta

journal homepage: www.elsevier.com/locate/bbabio

Flavodoxin: A compromise between efficiency and versatility in the electron transfer from Photosystem I to Ferredoxin-NADP$^+$ reductase

Guillermina Goñi [a], Beatriz Herguedas [a], Manuel Hervás [b], José R. Peregrina [a], Miguel A. De la Rosa [b], Carlos Gómez-Moreno [a], José A. Navarro [b], Juan A. Hermoso [c], Marta Martínez-Júlvez [a], Milagros Medina [a,*]

[a] Departamento de Bioquímica y Biología Molecular y Celular, Facultad de Ciencias and Instituto de Biocomputación y Física de Sistemas Complejos (BIFI), Universidad de Zaragoza, 50009-Zaragoza, Spain
[b] Instituto de Bioquímica Vegetal y Fotosíntesis, Universidad de Sevilla-CSIC, Sevilla, Spain
[c] Grupo de Cristalografía Molecular y Biología Estructural, Instituto Química-Física Rocasolano, Consejo Superior de Investigaciones Científicas, Serrano 119, 28006 Madrid, Spain

ARTICLE INFO

Article history:
Received 8 October 2008
Received in revised form 1 December 2008
Accepted 9 December 2008
Available online 24 December 2008

Keywords:
Ferredoxin-NADP$^+$ reductase
Flavodoxin
Protein–protein interaction
Electron transfer
Photosystem I
Transient interaction

ABSTRACT

Under iron-deficient conditions Flavodoxin (Fld) replaces Ferredoxin in *Anabaena* as electron carrier from Photosystem I (PSI) to Ferredoxin-NADP$^+$ reductase (FNR). Several residues modulate the Fld interaction with FNR and PSI, but no one appears as specifically critical for efficient electron transfer (ET). Fld shows a strong dipole moment, with its negative end directed towards the flavin ring. The role of this dipole moment in the processes of interaction and ET with positively charged surfaces exhibited by PSI and FNR has been analysed by introducing single and multiple charge reversal mutations on the Fld surface. Our data confirm that in this system interactions do not rely on a precise complementary surface of the reacting molecules. In fact, they indicate that the initial orientation driven by the alignment of dipole moment of the Fld molecule with that of the partner contributes to the formation of a bunch of alternative binding modes competent for the efficient ET reaction. Additionally, the fact that Fld uses different interaction surfaces to dock to PSI and to FNR is confirmed.

1. Introduction

Ferredoxin NADP$^+$ reductase (FNR) catalyses the electron transfer (ET) from Photosystem I (PSI) to NADP$^+$. In plants, electrons are transferred from PSI to FNR by Ferredoxin (Fd), but in most cyanobacteria and some algae, under iron deprivation, Flavodoxin (Fld) can substitute for Fd. Fd and Fld are different in size, sequence, folding and cofactors ([2Fe–2S] for Fd and FMN for Fld). However, both can function in the midpoint potential range ~−400 mV [1] and, alignment on the basis of their electrostatic potentials indicates overlapping of their strong negative potentials around their redox centres [2]. The surfaces of PSI and FNR where Fd and Fld bind contain mainly positive patches (Fig. SP1), suggesting that electrostatic forces will contribute to the complex formation step preceding ET [3–5].

In cyanobacteria PSI assembles as a trimer, each monomer containing 12 proteins and more than 100 cofactors [6]. Electrons flow from the P700 reaction centre through a series of carriers to reach the terminal [4Fe–4S] clusters, F_X, F_A and F_B. The PsaC, PsaD and PsaE subunits contribute to the positively charged solvent accessible stromal site of PSI (Fig. SP1A). The PsaC subunit binds F_A and F_B and cannot be deleted without loss of PSI activity; PsaD is important for electrostatic steering of Fd and Fld; and PsaE has been implicated in controlling lifetime and stabilisation of the PSI:Fd complex, in cyclic ET and/or in a ternary complex with FNR [5,7]. K35 from PsaC on the *Chlamydomonas reinhardtii* PSI [8], as well as K106 from PsaD [9–11] and R39 on PsaE in *Synechocystis* [12], play key roles in binding of the protein acceptor. The nature of several *Anabaena* Fld side chains has been shown to contribute to the formation of a transient PSI:Fld complex. However, replacements had minor effects on the ET process itself, and for some mutants mechanisms involving no-transient complex formation were as efficient as the WT one [4,13–15]. In *Anabaena* FNR, the surface around the FAD group presents patches of positively charged residues (Fig. SP1B). R16, K72, R264 and especially K75 are required as positively charged, while L76 and L78 must be hydrophobic, for the efficient interaction with both Fd and Fld [1,16–18]. Key counterpart residues to those were found on the Fd surface, namely F65 and E94 [16,17]. However, individual replacements of residues on the Fld surface indicated that they were not involved in crucial specific interactions with FNR [18–20].

Therefore, the interaction of Fld with its partners appears to be less specific than that of Fd. This is also suggested by docking models showing that Fld could orientate in different ways on the FNR surface without significantly altering the distance between the methyl groups of FAD and FMN and, keeping the molecular dipoles on FNR and Fld nearly collinear [21]. The parameters that regulate the Fld movement between its docking site on PSI and that on FNR during Fld-dependent

* Corresponding author. Tel.: +34 976762476; fax: +34 976762123.
E-mail address: mmedina@unizar.es (M. Medina).

0005-2728/$ – see front matter © 2008 Elsevier B.V. All rights reserved.
doi:10.1016/j.bbabio.2008.12.006

photosynthetic ET are further studied in this work. Residues, T12, E16, E20, E61, E67, D126 and D144 have been replaced with positively charged or neutral side chains. The cooperative action of these residues has been analysed in the E16K/E61K, E16K/D126K, E16K/E20K/D126K and E16K/E61K/D126K/D150K Flds. Finally, K2 and K3, residues producing one of the few accumulations of positive potential on the Fld surface, were simultaneously replaced by producing the K2A/K3A and K2E/K3E Flds. The effect of these mutations on the association and ET processes of Fld with PSI and FNR are discussed on the bases of the changes produced in the surface electrostatic potential and the dipole moment magnitude and orientation, as well as on the structural bases that regulate midpoint-reduction parameters.

2. Materials and methods

2.1. Site directed mutagenesis, protein expression and purification

Mutations at K2, K3, T12, E16, E20, E61, D126 and D150 were introduced into the pTrc99a plasmid encoding the *Anabaena* Fld gene by PCR-based site-directed mutagenesis using the Stratagene Quik-Change Kit (see Supplementary material, SP) [14]. Multiple mutations were sequentially introduced after several rounds of mutagenesis. Mutations were verified by DNA sequence analysis and MALDI-TOF mass spectrometry. WT and mutated pTrc99a-Fld plasmids were overexpressed in *Escherichia coli* TG1 strain. Recombinant *Anabaena* PCC 7119 WT FNR, WT Fld and mutated Flds were purified from LB cultures of IPTG-induced *E. coli* [14]. UV/Vis spectra and SDS-PAGE were used as purity criteria. *Anabaena* PCC 7119 PSI particles were obtained as described [22]. The P700 content in PSI samples was calculated from the photoinduced absorbance changes at 820 nm, ε=6.5 mM^{-1} cm^{-1}. Chlorophyll concentration was determined according to Arnon [23]. The chlorophyll/P700 ratio of the PSI preparation was 104/1. The same batches of PSI and proteins were used throughout this study.

2.2. Spectral analyses

UV–visible spectral measurements were carried out on a Kontron Uvikon 942, an Agilent HP 8453 or a Varian Cary 100 Bio spectrophotometer. Measurements were carried out at 25 °C in 50 mM Tris/HCl, pH 8.0. Extinction coefficients of Fld_{ox}s were determined as described [24]. Other extinction coefficients were; $\varepsilon_{FNRox,458\ nm}$=9.4 mM^{-1} cm^{-1}, $\varepsilon_{Cytcox,550\ nm}$=8.4 mM^{-1} cm^{-1} and $\varepsilon_{Cytcrd,550\ nm}$=29.5 mM^{-1} cm^{-1}. Stepwise anaerobic photoreduction of Flds was carried out in the presence of 2 μM 5-deazariboflavin (5-dRf) and 3 mM EDTA [13] and used to determine the percentage of maximum semiquinone stabilised and its extinction coefficient (see SP). Dissociation constants (K_d), extinction coefficient changes ($\Delta\varepsilon$) and free energy ($\Delta G°$) for complex formation between WT FNR_{ox} and the Fld_{ox} variants were obtained by difference absorption spectroscopy [14]. Fitting of the experimental data to the theoretical equation for a 1:1 complex allowed the calculation of K_d and $\Delta\varepsilon$. Errors in the determined K_d and $\Delta\varepsilon$ values were ±15%, and ±10% for $\Delta G°$. The FNR NADPH-cytochrome *c* reductase activity was assayed by using the Fld mutants as electron carrier from FNR to cytochrome *c* (Cytc) (Sigma) [25]. Errors in the estimated K_m and k_{cat} values were ±15% and ±10%, respectively.

2.3. Oxido-reduction potential determinations

Midpoint reduction potentials were determined in a protein solution combining potentiometric measurements of the oxido-reduction potential with optical measurements [13,15]. Experiments were carried out by photoreduction of ~40 μM Fld in the presence of 2 μM 5-dRf, 3 mM EDTA and ~2 μM of each mediator dye at 25 °C in 50 mM Tris/HCl pH 8.0, in an anaerobic cuvette, using a gold electrode and a saturated calomel electrode (details in SP). Errors in the $E_{ox/sq}$ and $E_{sq/hq}$ were estimated to be ±5 mV.

2.4. Fast kinetic stopped-flow measurements

Stopped-flow measurements were carried out under anaerobic conditions using an Applied Photophysics SX17.MV spectrophotometer [14]. Reduced samples of FNR and Fld were prepared by photoreduction. Reactions were followed after mixing the proteins at a ~1:1 molar ratio with a final concentration of ~10 μM for each protein, in 50 mM Tris/HCl pH 8.0 at 10 °C. Processes between FNR and Fld were followed at 600 nm and, those between Fld_{hq} and $Cytc_{ox}$ at 550 nm. The apparent observed rate constants (k_{ap}) were calculated by fitting the data to mono- or bi-exponential processes. Each kinetic trace was the average of 20–30 measurements. Each experiment was repeated three times. Maximal errors in the determined k_{ap} values were ±15%.

2.5. Fast kinetic laser-flash absorption spectroscopy measurements

ET processes between PSI and Fld were followed at 580 nm by laser-flash absorption spectroscopy [14]. The standard reaction mixture contained in 1 ml, 20 mM Tricine/KOH, pH 7.5, 0.03% β-dodecyl maltoside, an amount of PSI-enriched particles equivalent to 50 μg of chlorophyll ml^{-1}, 0.05 μM phenazine methosulfate, 2 mM $MgCl_2$, 2 mM sodium ascorbate, and Fld at the indicated concentration. The experiments at increasing $MgCl_2$ concentrations were carried out with a final Fld concentration of 20 μM. Each kinetic trace was the average of 40–50 measurements, with 30 s intervals between flashes. Observed rate constants (k_{obs}) were obtained from 2 to 3 different experiments and analyses were carried out according to the two-step reaction mechanism [14]. Error in the determination was <20%.

2.6. Crystal growth, data collection, and structure refinement

Crystals of K2A/K3A, E16K/E61K and E16K/E61K/D126K/D150K Flds were obtained by the hanging drop method: for K2A/K3A and E16K/E61K Fld, 1.5–2 μl of a 5 mg/ml protein solution in Tris/HCl pH 8.0 were mixed with 1 μl of reservoir solution consisting of 32% PEG 4000, 0.2–0.3 M $MgCl_2$ and 0.1 M Tris/HCl pH 8.5; for E16K/E61K/D126K/D150K Fld, 1 μl of a 5 mg/ml protein solution buffered with 0.1 M Tris/HCl pH 8.0 was mixed with 1 μl of reservoir solution consisting of 22% PEG 8000 and 0.2 M $CaCl_2$ buffered with 0.1 M MES, pH 6.5. The X-ray data set of the K2A/K3A Fld crystal was collected at the BM16 beamline of the ESRF on an ADSC Quantum210 detector with a wavelength of 0.97918 Å. Data for E16K/E61K and E16K/E61K/D126K/D150K Flds were collected with a Kappa 2000 CCD detector using a graphite monochromated CuK_α radiation generated by a Bruker–Nonius rotating anode. Data collection and refinement statistics are shown in Table SP1. The V_m are 1.95, 1.99 and 1.96 $Å^3$/Da and over 36.8%, 38.2% and 37.4% solvent contents for K2A/K3A, E16K/E61K and E16K/E61K/D126K/D150K Flds, respectively. Data were processed, scaled and reduced with HKL2000 [26]. The mutant structures were solved by molecular replacement, using the program MOLREP [27] and the native Fld_{ox} structure (PDB code 1flv). Refinement was made using the programs CNS [28] and REFMAC [29] and manual model building by the graphics program "O" [30]. In E16K/E61K Fld tight non-crystallographic restraints between the four different protein chains of the asymmetric unit were applied during refinement, which were gradually loosened in the final rounds. Stereochemistry of the models was checked using PROCHECK [31]. Atomic coordinates are deposited at the PDB: 3esz for K2A/K3A Fld, 3esy for E16K/E61K Fld and 3esx for E16K/E61K/D126K/D150K Fld.

2.7. Electrostatic potential surface and dipole moment calculations

In silico Fld mutant models, based on the *Anabaena* WT Fld structure (PDB 1flv), were generated using the mutation tool implemented in SPDB-Viewer 3.7 [32]. Energy minimization was done using the AMBER suite of molecular dynamics simulations and the amber force field [13,33]. The partial charge on each FMN atom was taken from [34]. The H++ server was used to protonate hydrolysable residues [35]. R.m.s.d. values for all atoms of modelled molecules with regard to WT were under 0.2 Å [13]. Molecular surfaces with electrostatic potential were calculated with PyMol [28]. The dipole moment (μ) for WT and mutated Flds was calculated by using the equation $\mu=\Sigma q_{iB} r_{iB}$; q_{iB} being the partial charge and r_{iB} the coordinates of each protein atom. The centre of mass of each protein was used as the reference position for calculation of μ [13].

3. Results

3.1. Expression, purification and spectral properties of the Fld mutants

Absorbance spectra of the Fld mutants were similar to those of WT Fld (Table SP2), indicating that they fold and bind FMN without major structural perturbations. The flavin extinction coefficients only slightly differed from that of the WT Fld, and changes were measurable only for the D144A Fld.

3.2. Midpoint reduction potentials

Flds containing individual charge reversal replacements at positions 12, 16, 20, 67 or 126, as well as the E16K/D126K and E16K/E20K/D126K multiple mutants, only produced minor effects on $E_{ox/sq}$ and $E_{sq/hq}$ (Table 1, Fig. 1). However, E61K, E16K/E61K and E16K/E61K/D126K/D150K displaced $E_{ox/sq}$ to considerably more negative values, whereas $E_{sq/hq}$ was less negative (Fig. 1). Such displacements explained the decrease in the amount of the maximal semiquinone stabilised by these mutants (Table SP2). Replacement of D144 with Ala produced a Fld with a $E_{sq/hq}$ considerably less negative than WT Fld. Again, this correlated with a considerably decrease in the maximal amount of semiquinone stabilised. Finally, simultaneous replacement of the N-terminal lysines with either Ala or Glu moderately influenced less negative $E_{ox/sq}$ values, but had not effect on $E_{sq/hq}$.

Table 1
Midpoint reduction potentials for the different *Anabaena* Fld forms

Fld form	$E_{ox/sq}$ (mV)	$E_{sq/hq}$ (mV)	$E_{ox/sq}-E_{ox/sq}^{WT}$ (mV)	$\Delta E_{stq/hq}-E_{sq/hq}^{WT}$ (mV)
WT[a]	−256	−445	–	–
T12K[b]	−252	−438	4	7
E16K[b]	−254	−440	2	5
E20K[a]	−265	−430	−9	15
E61K	−298	−399	−42	46
E67A	−258	−457	−2	−12
D126K	−254	−451	2	−6
D144A	−248	−375	8	70
E16K/E61K	−301	−390	−45	55
E16K/D126K	−253	−440	3	5
E16K/E20K/D126K	−255	−438	1	7
E16K/E61K/D126K/D150K	−297	−391	−41	54
K2A/K3A	−238	−445	18	0
K2E/K3E	−232	−444	24	1
FMN free[c]	−365	−117	−109	328

Data obtained in 50 mM Tris/HCl at pH 8.0 and 25 °C.
[a] Data were according to those previously published [15]. Reproducible WT data have been again obtained in the present work as control.
[b] Data from [13].
[c] Calculated as described [15,49] (pH 8.0 and 25 °C).

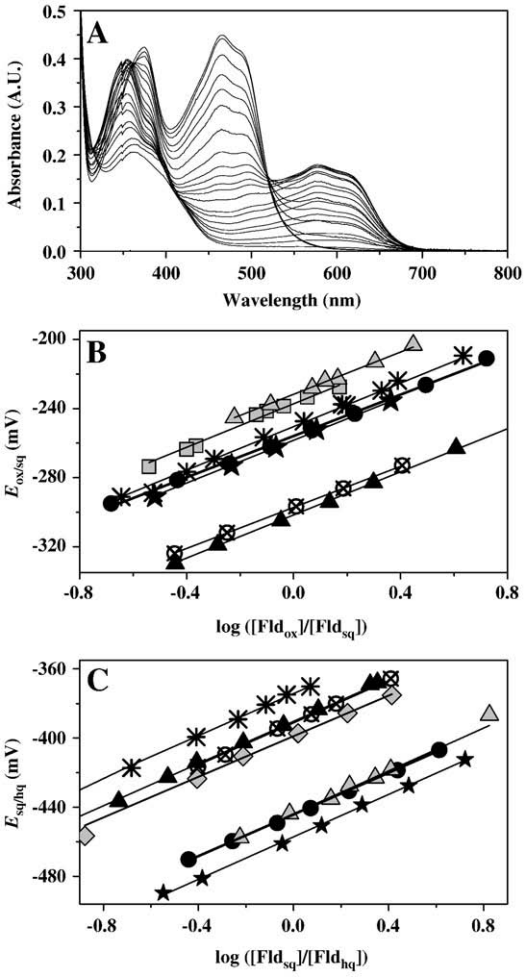

Fig. 1. (A) UV–visible spectra obtained during photoreduction and redox titration of the E16K/E61K/D126K/D150K Fld mutant. (B) Nernst plots for the different oxidised/semiquinone Fld forms: WT (black circles), E67A (black stars), D144A (asterisks), E16K/E61K (black triangles), E16K/E61K/D126K/D150K (crossed circles), K2A/K3A (light grey squares), K2E/K3E (light grey triangles). (C) Nernst plots for the different semiquinone/hydroquinone Fld forms: WT (black circles), E61K (light grey rhombi), E67A (black stars), D144A (asterisks), E16K/E61K (black triangles), E16K/E61K/D126K/D150K (crossed circles), K2E/K3E (light grey triangles).

3.3. Interaction of Fld_{ox} variants with FNR_{ox}

The spectral changes elicited upon titration of FNR_{ox} with the Fld_{ox} mutants were in general similar to those reported for the interaction of WT proteins. However, titrations with T12K and D144A showed displacements of the flavin Band-II (Fig. 2A, Table 2), suggesting slightly different environments for the FAD–FMN interaction [14]. No difference spectra were observed when titrating FNR with E16K/E20K/D126K or E16K/E61K/D126K/D150K Flds. Thus, combination of these mutations prevented the FNR–Fld interaction through their flavins. The E67A, D126K, K2A/K3A and K2E/K3E Flds interaction parameters with FNR were similar to those reported for WT Fld (Fig. 2B, Table 2). E20K, E61K and E16K/D126K mutations induced a slight weakening of the FNR_{ox}:Fld_{ox} interaction. 14- to 18-fold weaker complexes were observed with E16K and E16K/E61K Flds and, up to 23- and 36-fold weaker ones with T12K and D144A, respectively (Table 2). In general, extinction coefficient changes ($\Delta\varepsilon$) were within a factor of 2 of the WT Fld complex (Table 2). However, $\Delta\varepsilon$ slightly increased beyond that factor for the titration with D144A, while a decrease was observed for the double E16K/E61K and E16K/D126K mutants. These later observations suggest slightly different relative interactions between the flavin centres with regard to those found in the WT complex.

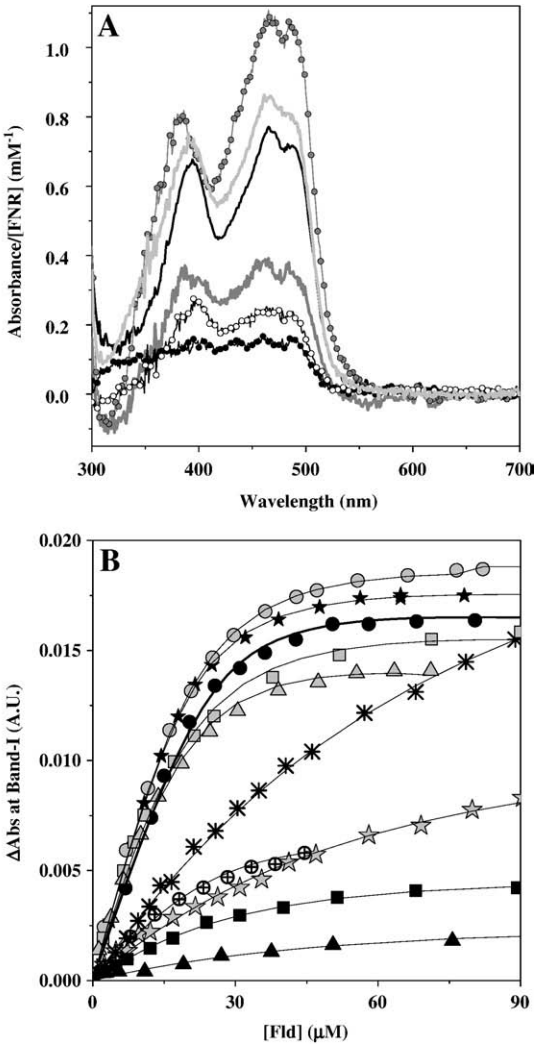

Fig. 2. Spectroscopic characterization of WT FNR_{ox}:Fld_{ox} complexes: (A) Difference absorption spectra elicited by the binding to WT FNR_{ox} of WT (bold black line), T12K (bold dark grey line), D144A (grey circles), E16K/E61K (black circles), E16K/D126K (white circles), K2A/K3A (bold light grey line) Fld_{ox}, (B) Titration of WT FNR with WT (black circles), T12K (light grey stars), E16K (crossed circles), E67A (black stars), D126K (light grey circles), D144A (asterisks), E16K/E61K (black triangles), E16K/D126K (black squares), K2A/K3A (light grey squares), K2E/K3E (light grey triangles) Fld. Fittings for a 1:1 interaction are shown.

3.4. Steady-state kinetic parameters for WT FNR when using the Fld mutants as electron carriers

The FNR cytochrome *c* reductase activity [25] was assayed using the different Flds to investigate whether the introduced mutations modulate the Fld ability to interact and to exchange electrons with FNR and Cytc (Table 2). E16K/E20K/D126K and E16K/E61K/D126K/D150K Flds presented low efficiency exchanging electrons between FNR and Cytc as consequence of very high K_m^{Fld} values. However, the use of D144A and E67A Flds slightly improved the FNR k_{cat} (Table 2), suggesting that these mutants have improved either their abilities as FNR electron acceptors and/or as Cytc electron donors. In general, the mutations produced larger K_m^{Fld} values, with the only exception of D126K Fld (Table 2). FNR K_m^{Fld} increased by a factor of 3-fold when using T12K, E67A, D144A and E16K/E61K Flds or 5-fold with E20K, E61K and E16K/D126K Flds. Combination of both effects produced significant differences in the FNR catalytic efficiency (k_{cat}/K_m) (Table 2), but the single D126K mutant was the only that led to an increased efficiency apparently due to the formation of stronger interactions. In conclusion, the use of E20K, E61K, E16K/D126K, E16K/E20K/D126K and especially E16K/E20K/D126K or E16K/E61K/D126K/D150K Flds considerably hindered the efficiency of the ET process from FNR to Cytc, most likely due to weaker productive interactions between these Fld variants and FNR.

3.5. Pre-steady-state kinetic analysis of the ET from Fld_{hq} mutants to $Cytc_{ox}$

To elucidate if changes observed in FNR catalytic efficiency could be due to a less efficient interaction and ET between Fld and Cytc, ET from the Fld_{hq} mutants to $Cytc_{ox}$ was analysed by stopped-flow. Similar two-exponential kinetics to those for the $Cytc_{ox}$ reduction by WT Fld were observed for the Fld mutants [18]. Processes with E16K, E67A, D126K, D144A, K2A/K3A and K2E/K3E Fld_{hq}s presented k_{ap} values within a factor of 2 of WT Fld_{hq} (Table 3), indicating that these residues do not play a major role in the optimal Cytc–Fld interaction. However, E16K/E61K, E16K/D126K, E16K/E20K/D126K and, especially T12K and E16K/E61K/D126K/D150K Fld_{hq}s transferred electrons to $Cytc_{ox}$ with slower rates (Table 3).

3.6. Pre-steady-state kinetic analysis of the ET processes between FNR and Fld mutants

When following the time course of the physiological ET reaction, from Fld_{hq} to WT FNR_{ox}, processes with T12K, E67A, D126K and K2E/K3E Flds showed WT behaviour (Table 3 and Fig. 3A and B). Kinetic traces for these reactions fit a two step process: formation of the semiquinones of both proteins, followed by further reduction of FNR_{sq} to the fully reduced state by a second Fld_{hq} molecule [14]. The reaction between the WT proteins takes place mainly within the instrumental dead time (~2 ms) and therefore, k_{ap2} cannot be separated from k_{ap1} [25]. However, the process was reported considerably slower for some mutants, allowing the determination of the two rate constants separately [14,20,25]. Processes with the remaining mutants were slower and different behaviours could be observed. The E16K and, particularly, the K2A/K3A Flds despite showing slower k_{ap1} and k_{ap2} parameters were still able to reduce FNR (Table 3, Fig. 3A and B). Combined charge reversal mutations around the FMN hindered ET from Fld_{hq} to FNR_{ox}, the effect being particularly patent in E16K/E61K/D126K/D150K Fld. The process was also hindered with D144A. The amplitudes of the kinetic traces were in general similar for the different Fld variants. The only exception was the reduction of FNR_{ox} by D144A Fld_{hq} that took place in considerably lower extent (Fig. 3A).

The reverse reaction, WT FNR_{hq} with WT Fld_{ox}, has been shown as a relatively slow two-step process due to initial production of Fld_{sq} and FNR_{sq}, followed by the reduction of a second Fld_{ox} molecule by the FNR_{sq} produced in the first step [14,20,25]. The kinetic traces for the reaction of all Fld_{ox} mutants also fit a biphasic process (Fig. 3C and D). In general, k_{ap1} values were within a factor of 2 of that with WT Fld_{ox}. However, E67A, E16K/E61K and, especially, T12K appear more efficient accepting electrons from FNR, while a hindering effect was observed for D144A, E16K/E126K and E16K/E61K/D126K/D150K (Table 3). k_{ap2} values were especially slower for E16K, D144A and the mutants containing simultaneous replacements of negatively charged residues. The amplitudes of the traces were in general similar or within a factor of 1.5 larger than those observed for the reaction with WT Fld_{ox}.

3.7. Pre-steady-state kinetic analysis of the reduction of Fld variants by PSI

Reduction of Fld_{ox} to the semiquinone state by PSI_{rd} using laser-flash absorption spectroscopy has demonstrated to be a useful model to analyse the interaction forces and ET parameters involved in the physiological reaction [5,13,14,20]. In addition, and although the Fld_{sq}/Fld_{hq} couple is with no doubt involved in shuttling electrons between PSI and FNR, a physiological role for the Fld_{ox}/Fld_{sq} couple

Table 2
Steady-state parameters for the *Anabaena* PCC 7119 Fld–FNR interaction

Fld form	K_d (μM)	$\Delta\varepsilon_{\text{band-I}}$ (M^{-1} cm^{-1})	Band-II (nm)	Band-I (nm)	$\Delta G°$ (kcal mol^{-1})	k_{cat}^{Fld} (s^{-1})	K_m^{Fld} (μM)	k_{cat}/K_m^{Fld} (μM^{-1} s^{-1})
WT[a]	2.6	1.5	394	465	−7.5	23.3	33.0	0.70
T12K	60	1.5	386	463	−5.8	24.9	78.6	0.32
T12V[b]	2.2	1.4	394	465	−7.8	11.0	11.1	1.00
E16K	37	1.2	394	464	−6.0	18.6	33.7	0.55
E20K[b]	14.5	2.4	394	465	−6.6	25.0	172	0.14
E61K[b]	11	2.9	394	465	−6.8	31.3	166	0.19
E67A	3.0	1.9	390	462	−7.5	65.5	97.9	0.67
D126K	4.2	2.1	390	464	−7.3	23.5	12.2	1.93
D144A	94	3.6	382	465	−5.5	58.2	90.1	0.65
E16K/E61K	46	0.4	398	460	−5.9	39.3	91.4	0.43
E16K/D126K	19	0.6	398	463	−6.4	24.8	171	0.14
E16K/E20K/D126K	[c]	[c]	[c]	[c]		[d]	[d]	[d]
E16K/E61K/D126K/D150K	[c]	[c]	[c]	[c]		[e]	>400[e]	[e]
K2A/K3A	5.3	2.0	392	465	−7.2	28.5	49.2	0.58
K2E/K3E	4.3	1.8	392	465	−7.2	22.4	32.0	0.70

Dissociation constants, extinction coefficient changes at band-I, position of flavin bands in the difference spectra and free energy for complex formation of WT FNR_{ox} with WT and mutated Fld_{ox} forms and kinetic parameters for the FNR NADPH-dependent cytochrome *c* reductase activity using the different Fld variants.

[a] Data were according to those previously published [25].

[b] Data from [20].

[c] Difference spectra were not observed.

[d] The dependence of the kinetic on [Fld] was linear with a $k = 5.0\times10^{-6} \pm 1.4\times10^{-7}$ μM^{-1} s^{-1}.

[e] Saturation could not be reached, the data only allowed estimation of a minimal K_m value.

cannot be precluded [5,7]. All Fld mutants showed monoexponential kinetic traces when reduced by PSI_{rd}, as reported for WT Fld [3]. The k_{obs} for the reduction of WT, T12K, E67A, E16K/E61K/D126K/D150K and K2A/K3A Fld_{ox}s depended non-linearly on the Fld concentration, showing a saturation profile (Fig. 4A and B). This suggests that a transient bimolecular PSI_{rd}:Fld_{ox} complex is formed prior to ET [4,36], although different explanations for this type of saturation profiles have also been given [37]. From the non-linear dependence of k_{obs} *vs* Fld concentration, minimal values for both the K_d and the ET first-order rate constant (k_{et}) can be inferred (Fig. 4A and B, Table 4). Replacement of T12 with Lys only slightly increased the affinity of Fld_{ox} by PSI_{rd}, but hindered its ability to accept electrons from PSI_{rd}. On the contrary, the simultaneous introduction of two Ala at K2 and K3 produced a 3-fold decrease of the complex affinity, but enhanced the ET rate. Noticeably, simultaneous replacement with Lys of positions 16, 61, 126 and 150 produced a Fld that accepts the electron twice faster (Fig. 4B, Table 4). The remaining mutants showed a linear dependence of k_{obs} on Fld concentration (Fig. 4A and B). This indicates that PSI_{rd} and these Fld_{ox} mutants reacted, under the assayed conditions, through a collisional type mechanism without detectable transient complex formation. Second order bimolecular rate constants (k_2) for Fld reduction can be estimated from the linear plots (Table 4). Although the observed linear dependences indicated that the equilibrium constant for complex formation was decreased, the k_{obs} values obtained at high Fld concentration were similar or even considerably higher (see the E16K/D126K, D144A and, particularly, E16K/E61K in Fig. 4A and B and Table 4) than those exhibited by WT Fld. In contrast, E16K/E20K/D126K Fld was unable to accept one electron from PSI (Fig. 4B, Table 4).

The k_{obs} profiles determined at varying $MgCl_2$ concentrations presented in general a biphasic dependence (Fig. 4C and D), as reported for the WT protein [3,14]. This bell-shaped salt dependence is explained as the initially formed electrostatic interaction being not the optimal for ET, requiring thus a rearrangement that could be prevented by the strong electrostatic forces acting at low ionic strength [3]. The E16K/E61K and E16K/E61K/D126K/D150K profiles indicate a shift of the maximum k_{obs} to a lower $MgCl_2$ concentration. Therefore, for these particular variants the most efficient orientation for ET is obtained at lower ionic strengths, at which higher efficiencies than for the WT are observed. Moreover, despite E16K/E20K/D126K Fld kept its low efficiency through the whole salt concentration range, it also showed a maximum at lower ionic strength than WT (Fig. 4D). On the contrary, k_{obs} for T12K Fld was considerably enhanced with increasing $MgCl_2$ concentrations, reaching similar values to WT Fld at the highest concentrations studied and showing a displacement of k_{obs} maximum to higher ionic strengths (Fig. 4C). These data suggest that T12K favours a strong non-productive interaction at low ionic strength, but it does not prevent Fld from accepting electrons from PSI when the strong electrostatic interaction is abolished.

3.8. Structures of the K2A/K3A, E16K/E61K and E16K/E61K/D126K/D150K Flds

The E16K/E61K Fld crystal structure had four Fld monomers in the asymmetric unit (Table SP1), which were overall similar among them (r.m.s.d. 0.40 Å for Cα) and with WT Fld (0.46, 0.44, 0.44 and 0.51 Å for A, B, C, and D monomers, respectively). Monomer A showed a *cis*-isomer of the N58-I59 peptide bond (Fig. SP2A), apparently due to the insertion of Tyr49, from a symmetry related monomer, between I59 and the isoalloxazine (Fig. SP2A). The conformation of the *cis*-bond was stabilised by a H-bond between the NH of residue 60 and a water molecule that bridges with the N5 of the isoalloxazine through a second H-bond. The crystal packing does not affect the conformation of this loop in B, C and D, which retain the *trans* isomer as in WT Fld. Nevertheless, the distance between the isoalloxazine N5 and the NH of I59 slightly differs among B, C and D monomers (between 3.30 and 3.68 Å).

E16K/E61K/D126K/D150K Fld presented two monomers in the asymmetric unit (Table SP1). None of the four replacements provoked a significant change in the Cα backbone configuration (r.m.s.d. with regard to WT Fld 0.45 and 0.66 Å for A and B monomers, respectively), despite the orientation of the introduced Lys chains was different from those of the replaced residues. These changes in orientation are often observed in residues facing the solvent. The conformation of the 50′s loop was conserved in the mutant, being the H-bond between the N5 atom of the isoalloxazine ring of FMN and the N atom of I59 0.16 Å shorter than in WT Fld (Fig. SP2B).

The K2A/K3A Fld structure contained two Fld monomers in the asymmetric unit (Table SP1). Both subunits presented a similar conformation between them (r.m.s.d. 0.39 Å) and with WT Fld (0.49 and 0.42 Å for A and B, respectively) (Fig. 5A). Monomer A presented a

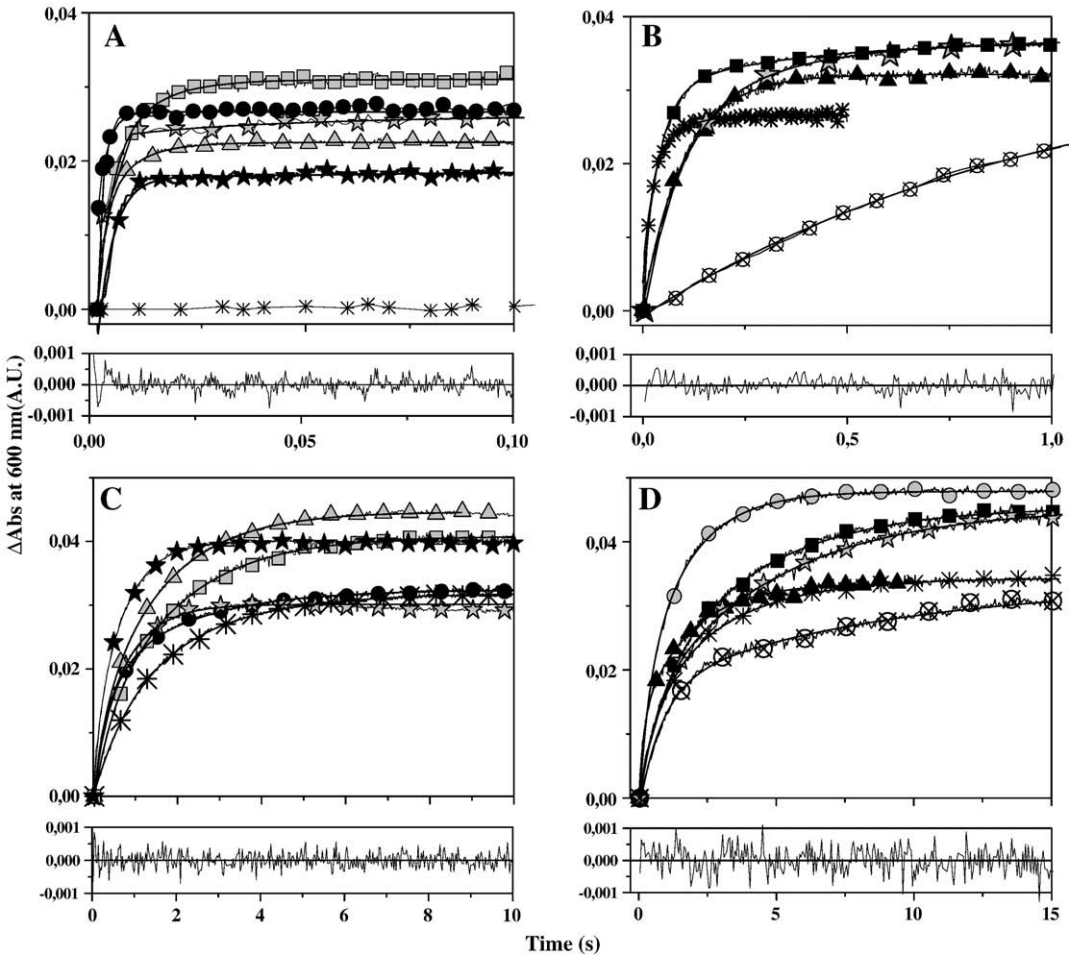

Fig. 3. Time course for the anaerobic reactions between WT FNR and selected Fld mutants measured by stopped-flow methodology and follow at 600 nm. Kinetic traces for the reactions of WT FNR_{ox} with (A) WT (black circles), T12K (light grey stars), E67A (black stars), D144A (asterisks), K2A/K3A (light grey squares), K2E/K3E (light grey triangles) Fld_{hq}, (B) E16K (asterisks), E16K/E61K (black triangles), E16K/D126K (black squares), E16K/E20K/D126K (light grey stars), E16K/E61K/D126K/D150K (crossed circles) Fld_{hq}. Residuals for fittings of the K2E/K3E and E16K/E20K/D126K Fld processes are shown at the bottom of the figures A and B, respectively. Kinetic traces for the reactions of WT FNR_{hq} with (C) WT (black circles), T12K (light grey stars), E67A (black stars), D144A (asterisks), K2A/K3A (light grey squares), K2E/K3E (light grey triangles) Fld_{ox}, (D) E16K (asterisks), D126K (light grey circles), E16K/E61K (black triangles), E16K/D126K (black squares), E16K/E20K/D126K (light grey stars), E16K/E61K/D126K/D150K (crossed circles) Fld_{ox}. Residuals for fittings of the D144A and E16K/E20K/D126K Fld processes are shown at the bottom of the Figures C and D, respectively.

cis disposition for the N58-I59 peptide bond that was not stabilised by any interaction between atoms of the 50′s loop and the N5 of the FMN isoalloxazine ring. In monomer B, the conformation of the 50′s loop remained essentially as in WT Fld. The H-bond between the isoalloxazine N5 and HN of I59 (3.34 Å) is shorter than in WT (3.71 Å). An additional consequence of the different configuration of 59–60 loop between monomers is that the NH of residue 60 in B is closer to the O4 atom of the isoalloxazine (2.74 Å, similar to that of WT Fld of 2.79 Å) than in A (3.04 Å).

4. Discussion

Fld must interact with PSI and FNR in such a way that its FMN cofactor faces towards the F_B [4S–4Fe] of PsaC in PSI or the FAD in FNR. The role of the Fld charge distribution in the optimal orientation of the protein, particularly of its FMN group, has been analysed.

4.1. Effects of mutations on the Fld midpoint potentials

$E_{ox/sq}$ was only considerably altered for E61K, E16K/E61K and E16K/E61K/D126K/D150K Flds (Table 1). This confirms replacement of E61 as the major determinant for the observed changes. Transition from the oxidised to the semiquinone in some Flds is accompanied by a backbone peptide rearrangement that provides a versatile device for $E_{ox/sq}$ manipulation [15,38]. In *Anabaena* Fld this corresponds to the 58–59 peptide bond. In the oxidised state the amide of I59 establishes a weak H-bond with the N5 of the flavin ring, "O-down" conformation. This bond is proposed to flip to an "O-up" conformation upon reduction to the semiquinone, involving the breaking of the above mentioned H-bond in favour of the formation of a stronger one between the carbonyl of N58 and N5H of FMN [13,38]. The more negative $E_{ox/sq}$ in E61K, E16K/E61K and E16K/E61K/D126K/D150K Flds are consistent with a less favourable thermodynamic conversion to the semiquinone (Table 1). The shorter N5-HN59 H-bond observed in these Fld_{ox}s (Fig. SP2), suggests an increase in the conformational energy of the N58-I59 bond that favours the "O-down" conformation. Therefore, E61 appears among the chains whose nature influences the "O-down to O-up" conformational change on one electron reduction of Fld_{ox}, making reduction more or less difficult and shifting $E_{ox/sq}$ to more or less negative values [13,15,19,39,40]. Surprisingly, the K2A/K3A and K2E/K3E Flds had slightly less negative $E_{ox/sq}$ values, despite their mutations being more than 30 Å away from FMN (Fig. 5B). However, they considerably decrease the magnitude of the Fld dipole moment changing also its direction (Fig. 6, Table SP3). The structure of K2A/K3A Fld also shows a possible relative orientation between the flavin and the 58–59 backbone that does not stabilise the H-bond with

Table 3
Fast kinetic parameters for the ET processes of *Anabaena* WT and mutated Fld forms with Cytc and WT FNR as determined by stopped-flow

Fld form	$Cytc_{ox}+Fld_{hq}$		$FNR_{ox}+Fld_{hq}$		$FNR_{hq}+Fld_{ox}$	
	k_{ap1} (s^{-1})	k_{ap2} (s^{-1})	k_{ap1} (s^{-1})	k_{ap2} (s^{-1})	k_{ap1} (s^{-1})	k_{ap2} (s^{-1})
WT	5.0	0.10	>600[a,c]	–[a]	2.5[a]	1.0[a]
T12K	0.8	0.02	>600[c]	–	13.5	1.3
T12V[b]	–	–	>600[c]	45	1.0	0.5
E16K	6.3	0.20	83	18	2.2	0.4
E20K[b]	–	–	>600[c]	245	15.5	1.3
E61K[b]	–	–	82	3.3	5.5	0.9
E67A	6.4	0.12	>340[c]	4.0	8.0	1.5
D126K	7.8	0.21	>600[c]	263	2.7	0.6
D144A	2.5	0.15	0.6	–	1.5	0.4
E16K/E61K	1.3	0.47	10	6.4	5.9	0.6
E16K/D126K	1.6	0.28	25	2.9	1.0	0.3
E16K/E20K/D126K	1.7	0.13	12	1.5	1.6	0.2
E16K/E61K/D126K/D150K	0.4	0.01	1.0	–	1.1	0.1
K2A/K3A	4.5	0.08	287	95	3.3	0.6
K2E/K3E	4.0	0.13	>470	127	2.7	0.5

[a] Data were according to those published [25].
[b] Data from [20].
[c] Most of the reaction occurred within the instrumental dead time.

the N5 of FMN (Fig. 5A, monomer A), thus favouring the reduction. Therefore, the structural flexibility in the 58–59 bond and the modulation of the distance between it and the N5 of the flavin support a function of this loop in the regulation of the $E_{ox/sq}$ in *Anabaena* Fld.

$E_{sq/hq}$ was in general not influenced by the introduced mutations (Table 1). However, in D144A, E61K, E16K/E61K and E16K/E61K/D126K/D150K $E_{sq/hq}$ shifted considerably. Since the FMN_{hq} in Fld is normally not protonated at N1, repulsive forces are generated in the negatively charged protein environment and electrostatic interactions are a determinant factor for the low $E_{sq/hq}$ [15,41]. The influence of charged residues depends on the distance and on the relative location to the isoalloxazine [15,19]. The decrease of the negative electrostatic potential around the flavin ring introduced by replacement of E61 (7 Å away from the ring) appears as the main cause of the displacement of $E_{sq/hq}$ to less negative values in E61K, E16K/E61K and E16K/E61K/D126K/D150K Flds (Fig. 5B). Replacement of D144 with Ala also had a remarkable effect on $E_{sq/hq}$. D144 contributes, together with D90, E145 and D146, to a negatively charged patch situated less than 6 Å from the isoalloxazine N1 (Fig. SP3). D144 is not solvent accessible or in direct contact with the flavin, but the electrostatic repulsion of its side chain appears to force those of D90 and D146 towards the isoalloxazine. Replacement of D144 with Ala must allow a retraction of D90 and D146 towards the position of D144 in WT Fld (Fig. SP3). This will allow a better neutralisation of the hydroquinone negative charge and therefore, a less negative $E_{sq/hq}$ [15]. Displacement of D90 and D146 chains might also increase the FMN solvent accessibility, a factor that contributes also to $E_{sq/hq}$ by making it less negative [15,42].

4.2. Effects of mutations on the Fld interaction and ET with FNR

The single mutations introduced at T12, E16, E67, D126 and D144, despite the negative influence on the interaction produced in some cases (T12K, E16K, D144A) (Table 2), generally allowed the exchange of

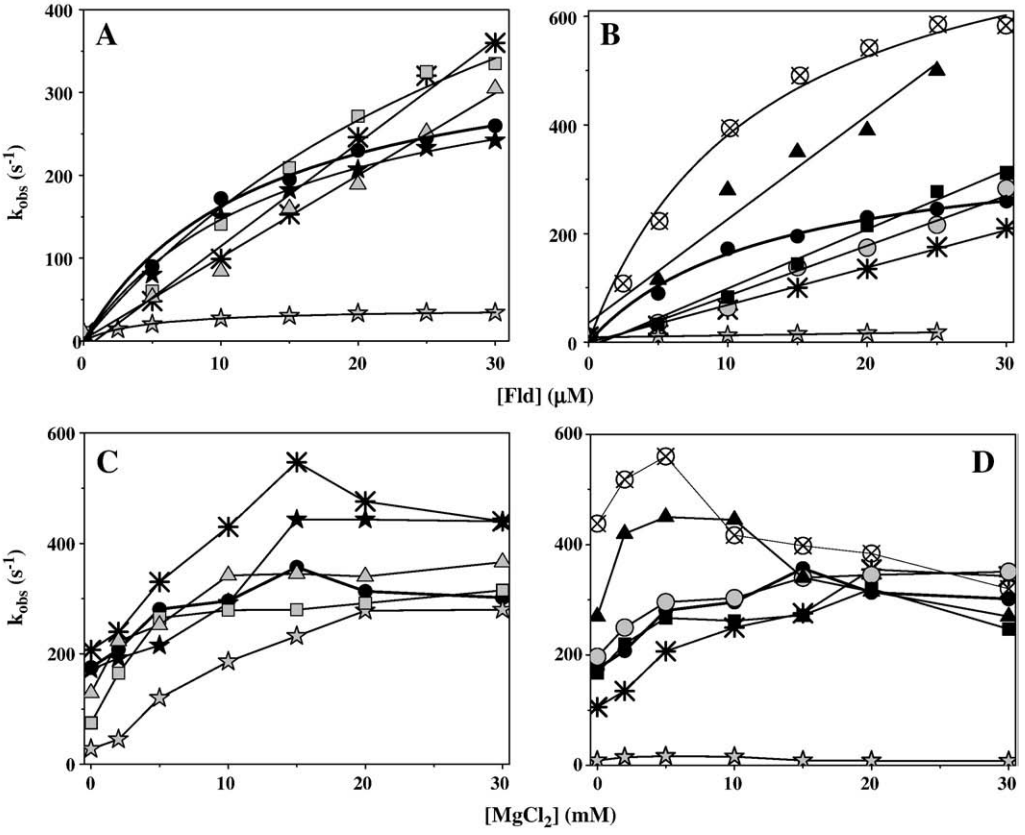

Fig. 4. Interaction and ET between WT and mutated Flds with WT PSI studied by laser flash-photolysis: Dependence of k_{obs} upon Fld concentration for reduction by PSI_{rd} of (A) WT (black circles), T12K (light grey stars), E67A (black stars), D144A (asterisks), K2A/K3A (light grey squares), K2E/K3E (light grey triangles) Fld_{ox} and, (B) WT (black circles), E16K (asterisks), D126K (light grey circles), E16K/E61K (black triangles), E16K/D126K (black squares), E16K/E20K/D126K (light grey stars), E16K/E61K/D126K/D150K (crossed circles) Fld_{ox}. Effect of $MgCl_2$ concentration on the k_{obs} for the reduction by PSI_{rd} of (C) WT (black circles), T12K (light grey stars), E67A (black stars), D144A (asterisks), K2A/K3A (light grey squares), K2E/K3E (light grey triangles) Fld_{ox} and (D) WT (black circles), E16K (asterisks), D126K (light grey circles), E16K/E61K (black triangles), E16K/D126K (black squares), E16K/E20K/D126K (light grey stars), E16K/E61K/D126K/D150K (crossed circles) Fld_{ox}.

Table 4
Kinetic parameters for the reduction of *Anabaena* WT and mutated Fld_{ox} forms by PSI_{rd} studied by laser flash-photolysis

Fld form	K_d (μM)	k_{et} (s^{-1})	k_2 ($\mu M^{-1}s^{-1}$)
WT	11.1	372	
T12K	4.3	39.5	
T12V[a]	10.0	130	
E16K	[b]	[b]	7
E20K[a]	[b]	[b]	3
E61K[a]	[b]	[b]	26
E67A	12.8	364	
D126K	[b]	[b]	9
D144A	[b]	[b]	12
E16K/E61K	[b]	[b]	19
E16K/D126K	[b]	[b]	11
E16K/E20K/D126K	[b]	[b]	0.4
E16K/E61K/D126K/D150K	9.1	848	
K2A/K3A	33.3	778	
K2E/K3E	[b]	[b]	10

The reaction was followed at 580 nm.
[a] Data from [20].
[b] The dependence of k_{obs} on [Fld] was linear.

electrons between Fld and FNR or Cytc (Tables 2 and 3). k_{cat} and k_{ap} values for these ET processes were in many cases modulated, either positively or negatively. Since these mutations did not produce major changes in the thermodynamics (Table 1), the kinetic effects must be due to the difference in the strength of the interaction, caused by small changes in their electrostatic surface potentials and in the orientation and magnitude of their molecular dipole moments (Fig. SP4, Table SP3). Therefore, these positions appear far from being critical by their own for the interaction and ET between Fld and FNR. The only exception is D144A Fld. This mutation prevents the physiological ET from Fld_{hq} to FNR (Table 3, Fig. 3). The explanation must be found in its $E_{sq/hq}$ that makes the ET from Fld_{hq} to FNR much less favourable from the thermodynamic point of view.

Among the mutants produced by simultaneous replacements at E16, E61, D126 or D150, only E16K/E61K and E16K/D126K produced complexes with FNR. The strength of these interactions was similar to that of the single E16K variant, but $\Delta\varepsilon$ suggests considerably smaller degrees of interaction between the flavins (Fig. 2, Table 2). These Flds appear still able to accept electrons from FNR (Table 3, Fig. 3), but the decrease in the strength of the interaction with FNR and in the ET efficiency with Cytc makes them poor electron carriers (Tables 2 and 3). Additionally, all these mutants, but particularly E16K/E61K/D126/D150K, have lost the ability to efficiently reduce FNR (Table 3). More positive $E_{sq/hq}$ values might somehow contribute to the behaviour of E16K/E61K and E16K/E61K/D126/D150K Flds, but not to the other two mutants. Important changes in their electrostatic potential surfaces are observed, which influence changes in the orientation and magnitude of their molecular dipole moments (Table SP3, Figs. 5B and 6). Thus, while in WT Fld and the single mutants the negative end of the dipole moment points towards the flavin ring, the negative end of E16K/E61K/D126/D150K is not anymore oriented towards it (Fig. 6A). In fact, if docking between this mutant and FNR would still have to occur through the alignment of their respective dipole moments, this mutant would never face the FAD cofactor of FNR through its FMN surface (Fig. 6B and C). This is consistent with the lack of interaction between FMN and FAD observed when titrating FNR with this mutant. Surprisingly, as above mentioned, these Flds were still able to accept electrons from FNR. Despite that the thermodynamic parameters favour the process, the observed reaction might only correlate with a collisional-type reaction. This agrees with the proposal of alternative productive binding modes between FNR and Fld [19,21].

K2A/K3A and K2E/K3E Flds have an almost WT behaviour, the only difference being the slightly reduced k_{ap} when accepting electrons from FNR (Table 3). Minor effects should be expected from the

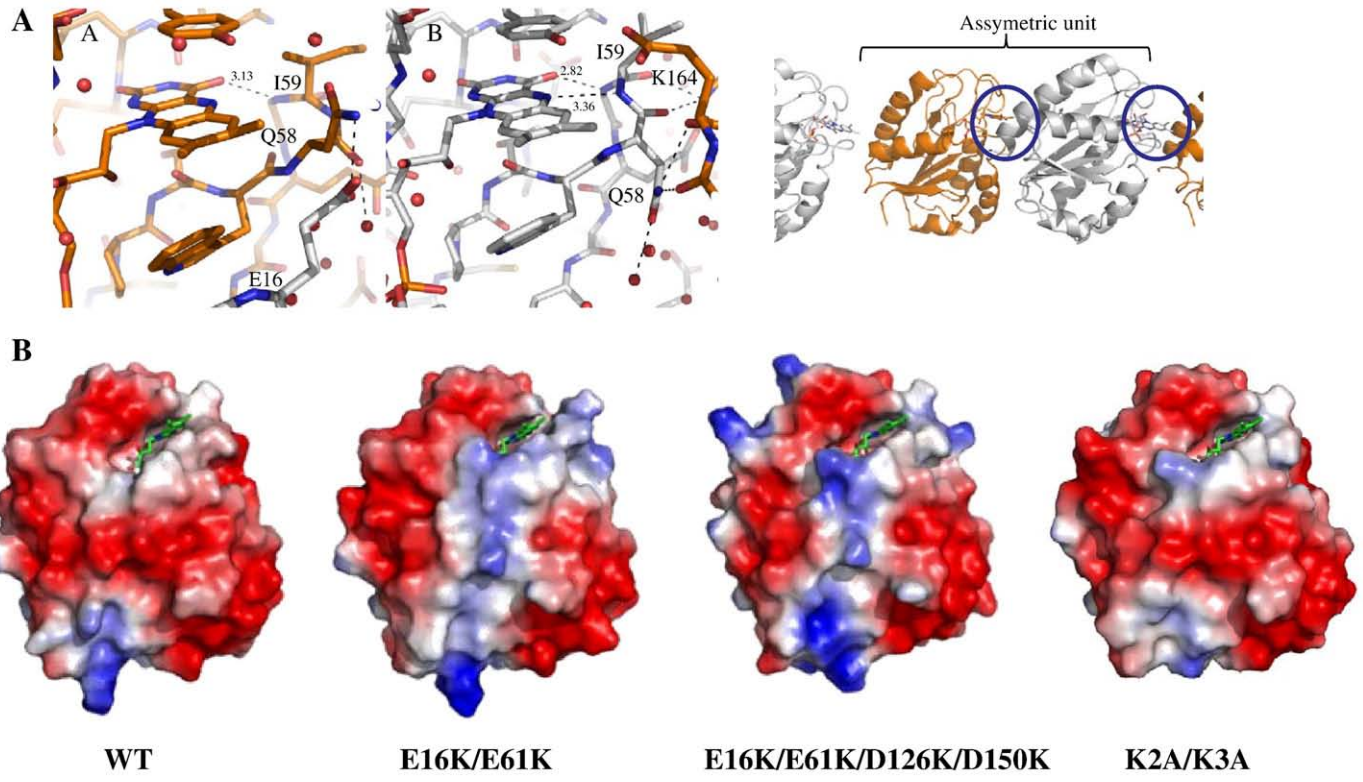

Fig. 5. (A) Detail of the FMN environment in the two monomers of the K2A/K3A Fld contained in their asymmetric units. CPK with C in different colours. Relevant H-bonds are shown in dotted lines. (B) Molecular surfaces with electrostatic potentials for the X-ray structures of WT, E16K/E61K, E16K/E61K/D126K/D150K and K2A/K3A Flds. The FMN group is shown in sticks and CPK coloured with C in green.

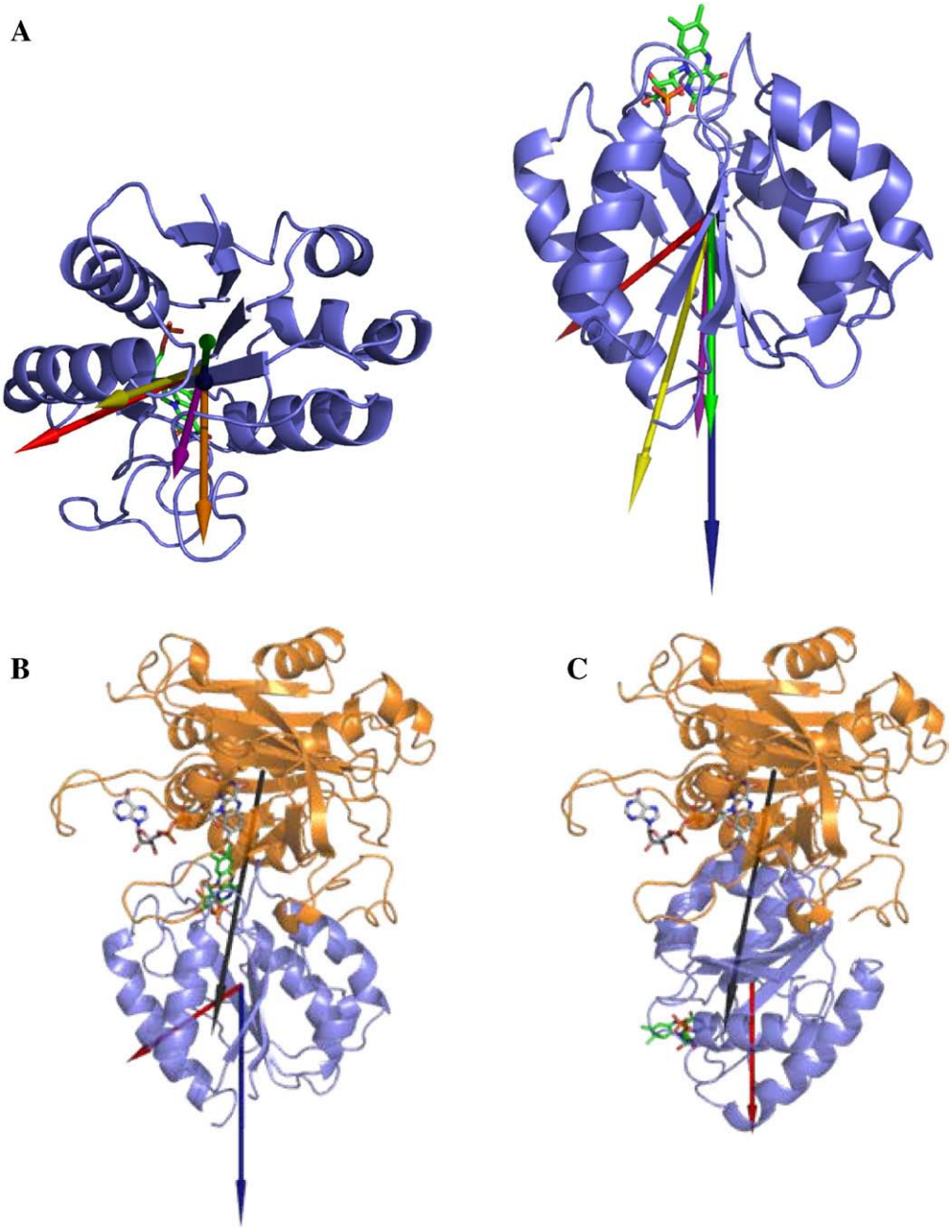

Fig. 6. (A) Magnitude and orientation of the dipole moments of K2A/K3A (violet arrow), K2E/K3E (orange arrow), E16K/D126K (yellow arrow), E16K/E61K/D126K/D150K (red arrow) and E16K/E61K (green arrow) Fld structures with regard to that of WT Fld (blue arrow). Two views rotated by 90° are shown. (B) Relative orientation of the molecular dipole moment of E16K/E61K/D126K/D150K Fld (red arrow) on the model for the docking interaction between FNR and Fld, dipoles for FNR and Fld are shown as black and blue arrows, respectively. (C) Model of the putative interaction of FNR and E16K/E61K/D126K/D150K Fld with a collinear orientation of their molecular dipole moments, but showing a relative disposition between the flavin rings not compatible with ET. Proteins are shown in blue cartoon for Fld and orange cartoon for FNR. The FMN and FAD groups are shown as sticks and CPK coloured with C in green and grey, respectively.

reaction thermodynamic driving force (Table 1). The explanation should be again found in the decrease of the Fld dipole moment magnitude and the change in its direction towards the FMN phosphate group (Fig. 6).

4.3. Effects of mutations on the ET from PSI to Fld

For many of the mutants ET from PSI_{rd} to Fld_{ox} takes place through a collisional-type mechanism (Table 4, Fig. 4). These data indicate that E16, D126 and D144 play some role in the formation of ET complexes with PSI. Noticeably, the k_{obs} values for E16K/E61K are higher than those obtained for WT (Fig. 4). This was already described when producing single mutants at E61 [20]. It indicates that E61 contributes to the orientation of Fld on the PSI docking site, producing a WT complex that is not the optimal for ET. For the rest of the mutations k_{obs} at a given concentration is lower than for WT Fld. Since the introduced mutations are not in the direct coordination of the isoalloxazine this can hardly be the consequence of a different structural FMN environment affecting the ET mechanism, but rather due to an orientation between the protein dipoles not optimal for ET or, to the change in the protein electrostatic potential (Figs. 5B and 6).

T12K, E67A, E16K/E61K/D126K/D150K and K2A/K3A Flds accept electrons from PSI following transient complex formation [3,14]. The

PSI_{rd}:T12K Fld_{ox} complex, despite being stronger than that for WT Fld, is not optimal for ET. Introduction of a Lys at position 12 is not expected to influence the orientation of the molecular dipole moment, but will induce changes in the electrostatic potential favouring a complex less efficient for ET (Fig. SP4). Similar results were reported when replacing T12 with Val, suggesting this Thr as a key residue in this process [20]. Binding ability of E16K/E61K/D126K/D150K Fld to PSI is not sensibly affected, but k_{et} is considerably enhanced. The more negative $E_{ox/sq}$ of E16K/E61K/D126K/D150K Fld (−41 mV) might influence its kinetic behaviour by decreasing the driving force of its reduction. The change in the orientation of the molecular dipole moment (Fig. 6) is expected to have also a negative effect. Complex formation with PSI is slightly impaired in K2A/K3A Fld mutant, but the k_{et} for its reduction is again enhanced (Table 4). This region of Fld is not expected to be involved in the interaction with PSI and the differences cannot be due to changes in the isoalloxazine environment. However, removal of these two Lys considerably reduced the magnitude of the Fld dipole moment and changes its orientation (Fig. 6, Table SP3). Therefore, the increased efficiency of E16K/E61K/D126K/D150K and K2A/K3A Flds in accepting electrons from PSI has to be related to different orientations of these Flds at the donor site of PSI. The exact localisation of the protein acceptor on the PSI is still far to be determined. Moreover, the orientation of the protein carrier on the PSI docking site might be different in plants and cyanobacteria. Additionally, PSI in cyanobacteria has also different arrangements when grown under iron deficient conditions [43]. Therefore, *in vivo* a variability of these interactions will be also occurring.

4.4. Electrostatic non-specific interactions as major determinants of the efficient interaction between Fld and its counterparts

The Fld interaction with FNR is confirmed to be less specific than that of Fd, and apparently more than one orientation in the encounter complex can be efficient. Additionally, some of the specific introduced mutations in Fld favour single orientations which improve association and ET with a particular partner. This suggests that the flavin atoms might be those mainly involved in the interaction, as suggested by docking analysis [21], and probably the only ones directly responsible for ET. Subtle changes at the isoalloxazine environment influence the Fld binding abilities and modulate the ET processes by producing different orientations and distances between the redox centres. This confirms that Fld interacts with different structural partners through non-specific interactions. This promiscuity, in turn decreases the potential efficiency in ET that could be achieved if unique favourable orientations were produced with a reduced number of partners [19]. Heterogeneity of ET kinetics is an intrinsic property of Fld reduction, and can be most probably ascribed to different conformations of the PSI:Fld and FNR:Fld complexes [5,21]. Therefore ET reactions involving Fld might not have as much specific interaction requirements as other reactions involving protein–protein interactions and, the bound state could be formed by dynamic ensembles instead of single conformations as has already been observed in other ET systems [44,45]. During Fld-dependent photosynthetic ET, the Fld molecule must pivot between its docking site on PSI to that on FNR. Formation of transient complexes is useful during this process, though not critical, for promoting efficient reduction of Fld and FNR and for avoiding reduction of oxygen [5,19]. The electrostatic alignment appears as one of the major determinants of the orientation of Fld on the partner surfaces. Fld-domains and FNR-domains in dual-flavin reductases appear to have eliminated the pressure to maintain strong contacts and the dipole moment alignment between the domains [46–48]. However, the negatively charge residues analysed in this work are also conserved in their Fld-domains (Fig. SP1C). Part of the role of these residues might have been conserved upon evolution to orientate the Fld-domain when pivoting between the FNR-domain and their electron acceptors [47]. Finally, the fact that the same replacements on the Fld surface did not similarly hinder or enhance processes with PSI and FNR also suggests a different interaction mode with both partners. Such modes can differ in the Fld surfaces in contact with both protein partners. These assumptions are also justified by considering the large number of negative charges borne by Fld, which should make its electrostatic steering on the positively charged FNR and, particularly, on the large PSI docking site, relatively insensitive to small changes in the Fld charge.

Acknowledgments

This work has been supported by the Spanish Ministry of Education and Science (BIO2007-65890-C02-01 to M.M.) and DGA (Grant PM062/2007 to M.M.). We thank Dr. JM Mancheño for his helpful assistance during X-ray data collection at the BM16 beamline of the ESRF.

Appendix A. Supplementary data

Supplementary data associated with this article can be found, in the online version, at doi:10.1016/j.bbabio.2008.12.006.

References

[1] M. Medina, C. Gómez-Moreno, Photosynth. Res. 79 (2004) 113–131.
[2] G.M. Ullmann, M. Hauswald, A. Jensen, E.W. Knapp, Proteins 38 (2000) 301–309.
[3] M. Medina, M. Hervás, J.A. Navarro, M.A. De la Rosa, C. Gómez-Moreno, G. Tollin, FEBS Lett. 313 (1992) 239–242.
[4] J.A. Navarro, M. Hervás, C.G. Genzor, G. Cheddar, M.F. Fillat, M.A. de la Rosa, C. Gómez-Moreno, H. Cheng, B. Xia, Y.K. Chae, et al., Arch. Biochem. Biophys. 321 (1995) 229–238.
[5] P. Sétif, Biochim. Biophys. Acta 1507 (2001) 161–179.
[6] P. Jordan, P. Fromme, H.T. Witt, O. Klukas, W. Saenger, N. Krauss, Nature 411 (2001) 909–917.
[7] P. Sétif, in: J.H. Golbeck (Ed.), Photosystem I. The Light-driven Platocyanin: ferredoxin Oxidoreductase, Springer, Dordrecht, The Netherlands, 2006, pp. 439–454.
[8] N. Fischer, M. Hippler, P. Sétif, J.P. Jacquot, J.D. Rochaix, EMBO J. 17 (1998) 849–858.
[9] J. Hanley, P. Sétif, H. Bottin, B. Lagoutte, Biochemistry 35 (1996) 8563–8571.
[10] V.P. Chitnis, Y.S. Jungs, L. Albee, J.H. Golbeck, P.R. Chitnis, J. Biol. Chem. 271 (1996) 11772–11780.
[11] P. Barth, I. Guillouard, P. Sétif, B. Lagoutte, J. Biol. Chem. 275 (2000) 7030–7036.
[12] N. Krauss, W. Hinrichs, I. Witt, P. Fromme, W. Pritzkow, Z. Dauter, C. Betzel, K.S. Wilson, H.T. Witt, W. Saenger, Nature 361 (1993) 326–331.
[13] S. Frago, G. Goñi, B. Herguedas, J.R. Peregrina, A. Serrano, I. Pérez-Dorado, R. Molina, C. Gómez-Moreno, J.A. Hermoso, M. Martínez-Júlvez, S.G. Mayhew, M. Medina, Arch. Biochem. Biophys. 467 (2007) 206–217.
[14] J.L. Casaus, J.A. Navarro, M. Hervás, A. Lostao, M.A. De la Rosa, C. Gómez-Moreno, J. Sancho, M. Medina, J. Biol. Chem. 277 (2002) 22338–22344.
[15] I. Nogués, L.A. Campos, J. Sancho, C. Gómez-Moreno, S.G. Mayhew, M. Medina, Biochemistry 43 (2004) 15111–15121.
[16] J.K. Hurley, R. Morales, M. Martínez-Júlvez, T.B. Brodie, M. Medina, C. Gómez-Moreno, G. Tollin, Biochim. Biophys. Acta 1554 (2002) 5–21.
[17] R. Morales, M.H. Charon, G. Kachalova, L. Serre, M. Medina, C. Gómez-Moreno, M. Frey, EMBO Rep. 1 (2000) 271–276.
[18] I. Nogués, M. Martínez-Júlvez, J.A. Navarro, M. Hervás, L. Armenteros, M.A. de la Rosa, T.B. Brodie, J.K. Hurley, G. Tollin, C. Gómez-Moreno, M. Medina, Biochemistry 42 (2003) 2036–2045.
[19] G. Goñi, A. Serrano, S. Frago, M. Hervás, J.R. Peregrina, M.A. De la Rosa, C. Gómez-Moreno, J.A. Navarro, M. Medina, Biochemistry 47 (2008) 1207–1217.
[20] I. Nogués, M. Hervás, J.R. Peregrina, J.A. Navarro, M.A. de la Rosa, C. Gómez-Moreno, M. Medina, Biochemistry 44 (2005) 97–104.
[21] M. Medina, R. Abagyan, C. Gomez-Moreno, J. Fernandez-Recio, Proteins 72 (2008) 848–862.
[22] M. Hervás, J.M. Ortega, J.A. Navarro, M.A. De la Rosa, H. Bottin, Biochim. Biophys. Acta 1184 (1994) 235–241.
[23] D.I. Arnon, Plant Physiol. 24 (1949) 1–15.
[24] S.G. Mayhew, V. Massey, J. Biol. Chem. 244 (1969) 794–802.
[25] M. Medina, M. Martínez-Júlvez, J.K. Hurley, G. Tollin, C. Gómez-Moreno, Biochemistry 37 (1998) 2715–2728.
[26] Z. Otwinowski, W. Minor, Methods Enzymol. 276 (1997) 307–326.
[27] A. Vagin, A. Teplyakov, J. Appl. Cryst. 30 (1997) 1022–1025.
[28] A.T. Brunger, P.D. Adams, G.M. Clore, W.L. DeLano, P. Gros, R.W. Grosse-Kunstleve, J.S. Jiang, J. Kuszewski, M. Nilges, N.S. Pannu, R.J. Read, L.M. Rice, T. Simonson, G.L. Warren, Acta Crystallogr. D. Biol. Crystallogr. 54 (1998) 905–921.

[29] G.N. Murshudov, A.A. Vagin, E.J. Dodson, Acta Crystallogr. D. Biol. Crystallogr. 53 (1997) 240–255.
[30] T.A. Jones, J.Y. Zou, S.W. Cowan, M. Kjeldgaard, Acta Crystallogr. A 47 (Pt 2) (1991) 110–119.
[31] R.A. Laskowski, M.W. MacArthur, D.S. Moss, J.M. Thornton, J. Appl. Cryst. 26 (1993) 283–291.
[32] N. Guex, M.C. Peitsch, Electrophoresis 18 (1997) 2714–2723.
[33] D.A. Case, T.E. Cheatham, T. Darden, H. Gohlke, R. Luo, K.M. Merz, A. Onufriev, C. Simmerling, B. Wang, R.J. Woods, J. Comput. Chem. 26 (2005) 1668–1688.
[34] C. Schneider, J. Suhnel, Biopolymers 50 (1999) 287–302.
[35] J. Myers, G. Grothaus, S. Narayanan, A. Onufriev, Proteins 63 (2006) 928–938.
[36] U. Muhlenhoff, P. Sétif, Biochemistry 35 (1996) 1367–1374.
[37] D.M. Tiede, A.C. Vashishta, M.R. Gunner, Biochemistry 32 (1993) 4515–4531.
[38] M. Kasim, R.P. Swenson, Biochemistry 40 (2001) 13548–13555.
[39] M.L. Ludwig, K.A. Pattridge, A.L. Metzger, M.M. Dixon, M. Eren, Y. Feng, R.P. Swenson, Biochemistry 36 (1997) 1259–1280.
[40] W. Watt, A. Tulinsky, R.P. Swenson, K.D. Watenpaugh, J. Mol. Biol. 218 (1991) 195–208.
[41] Z. Zhou, R.P. Swenson, Biochemistry 35 (1996) 15980–15988.
[42] R.P. Swenson, G.D. Krey, Biochemistry 33 (1994) 8505–8514.
[43] J. Nield, E.P. Morris, T.S. Bibby, J. Barber, Biochemistry 42 (2003) 3180–3188.
[44] J.A. Worrall, W. Reinle, R. Bernhardt, M. Ubbink, Biochemistry 42 (2003) 7068–7076.
[45] P.B. Crowley, M.A. Carrondo, Proteins 55 (2004) 603–612.
[46] M. Wang, D.L. Roberts, R. Paschke, T.M. Shea, B.S. Masters, J.J. Kim, Proc. Natl. Acad. Sci. U. S. A. 94 (1997) 8411–8416.
[47] K.R. Wolthers, X. Lou, H.S. Toogood, D. Leys, N.S. Scrutton, Biochemistry 46 (2007) 11833–11844.
[48] E.D. Garcin, C.M. Bruns, S.J. Lloyd, D.J. Hosfield, M. Tiso, R. Gachhui, D.J. Stuehr, J.A. Tainer, E.D. Getzoff, J. Biol. Chem. 279 (2004) 37918–37927.
[49] S.G. Mayhew, Methods Mol. Biol. 131 (1999) 49–59.

Glossary

ET: electron transfer
Fd: Ferredoxin
Fld, Fld_{ox}, Fld_{sq}, Fld_{hq}: Flavodoxin and in its oxidised, semiquinone and hydroquinone states, respectively
FNR, FNR_{ox}, FNR_{sq}, FNR_{hq}: Ferredoxin-$NADP^+$ reductase and in its oxidised, semiquinone and hydroquinone states, respectively
ApoFld: apoflavodoxin
K_d: dissociation constant
K_{ap}: apparent rate constant
K_{et}: first-order electron transfer rate constant
K_{obs}: pseudo first-order observed rate constant
K_2: second order rate constant
PSI, PSI_{ox}, PSI_{rd}: Photosystem I and in its oxidised and reduced states, respectively
WT: wild-type
Cytc, $Cytc_{ox}$, $Cytc_{rd}$: horse heart Cytochrome c and in its oxidised and reduced states, respectively